# A MIXED DOPPLER SHIFT AND POLARIZATION MANAGEMENT APPROACH FOR SATELLITE COMMUNICATIONS

BOUALEM NASRI, EL HABIB BENSIKADDOUR, AMINE BAB, SAIAH BEKKAR DJELLOUL SAIAH, DJAMEL EDDINE BABA HAMED, AKRAM ADNANE

Keywords: ALSAT-2A satellite; ALSAT-2B satellite; CDM 600 application; Doppler shift; Estimated Doppler shift.

The rapid displacement of satellites in low Earth orbit (LEO) poses several challenges for communication with the ground segment. One of the main problems encountered is significant Doppler frequency shifts, which can disrupt signal transmission and require precise adjustments to maintain stable communications. This paper presents a software solution to effectively compensate for the Doppler shift, along with a hardware implementation to manage the two available polarizations at the station: right-hand circular polarization (RHCP) and left-hand circular polarization (LHCP). This polarization management is necessary because the demodulator used in our case possesses only a single input. This solution has been implemented in an existing S-band ground station (GS) located in Oran, Algeria. The experimental results obtained during actual passes of the ALSAT-2A and ALSAT-2B satellites, whose orbits are 180 degrees apart, were satisfactory. The implemented solution showed good results, with an accuracy comparable to that of the estimated Doppler frequency, without any loss of telemetry at the ground segment level.

#### 1. INTRODUCTION

The ALSAT-2A and ALSAT-2B satellites, launched in low Earth orbit (LEO) in June 2010 and September 2016, respectively, are currently in service and positioned 180 degrees from each other. One of their main challenges is the accurate measurement of the Doppler shift resulting from their relative motion with the ground station (GS) [1]. A significant shift can degrade communication quality, leading to telemetry data loss and reduced orbit determination accuracy. Moreover, it can negatively impact the satellite's attitude control system [2,3], potentially leading to the loss of tracking [4]. To prevent these problems, it is essential to compensate for this offset so that ground transceivers can adjust for Doppler-related errors [5, 6].

In recent decades, several studies have concentrated on the satellite segment, with particular emphasis on the design and optimization of patch antennas to enhance signal quality and improve communication performance [7,8]. At the same time, much of the research has focused on estimating the Doppler shift for satellites in circular orbits by exploiting temporal data from Doppler observations made from points on the equator [9-12]. In this context, various satellite tracking techniques, such as Monopulse [13] and the step technique with  $H_{\infty}$  controller [14], have been developed. The authors of reference [15] propose a strategy to compensate for the Doppler shift in LEO communication systems by integrating a maximum likelihood Doppler estimator in the receiver. A software solution could be integrated into the satellite tracking system to calculate the Doppler shift. This shift is determined from the orbital two-line elements (TLE) and practical data collected by the station demodulator [16, 17]. The authors of [4] propose an approach to accurately predict the frequency Doppler shift in a LEO constellation operating in the L band. This approach is based on the value observed at the maximum elevation angle, as well as on the GS and satellite coordinates. A Doppler rate estimation algorithm is proposed by [18] to optimize the use of LoRa technology in satellite communications in low Earth orbit, when the Eb/N0 ratio exceeds 4 dB. In [19], the authors present a new approach using stochastic geometry to capture the statistical distribution of Doppler shifts in modern megasatellite constellations in LEO. The authors of [20] developed a hardware solution based on the ATmega 328

microcontroller to estimate the Doppler shift for LEO satellites. This solution was validated on the ALSAT-2A satellite.

In this paper, we present the results of the new experiments, in line with our previous work in [17, 20]. The basic architecture of the Oran S-band station uses both righthand circular polarization (RHCP) and left-hand circular polarization (LHCP) simultaneously. However, integrating new hardware components into this dual-polarization setup is not straightforward. Integrating a new demodulator, such as the CDM-600 from Comtech EF Data [21], into the existing architecture requires several development steps, as the new equipment has only a single input for demodulation. The first step of our work was the implementation of a module for managing the two polarizations, in which a microcontroller controls a radio frequency (RF) switch to select the optimal polarization for the single input of the CDM-600. The second step involved developing an application to configure the demodulator for the ALSAT-2 missions. Once this stage was completed, attention was directed to calculating the Doppler shift, which relies on comparing the theoretical and practical shifts. This calculation also requires adjusting the reference frequency once the measured offset reaches the limit of the required scan range, following demodulator locking tests.

The organization of this paper is as follows: Section 2 presents parameter definitions. Section 3 describes the proposed architecture. Section 4 discusses the implementation and the results obtained. Finally, Section 5 concludes the paper.

# 2. PARAMETER DEFINITION

#### 2.1 AZIMUTH AND ELEVATION

Azimuth and elevation are critical parameters that describe a satellite's position in the sky relative to an observer on Earth. These angles are especially important for tracking and communicating with LEO satellites, which orbit the Earth at altitudes typically between 160 and 2,000 kilometers [22].To calculate the azimuth, elevation, and range of a satellite from a GS perspective, we need to convert the satellite's position from Earth-centered, Earth-fixed (ECEF) coordinates to the local east-north-up (ENU) coordinate system, then compute the angles and distance (Fig. 1).

<sup>&</sup>lt;sup>1</sup> Satellite Development Center, POS 50 Ilot T12, Bir El-djir, Oran, Algeria.

E-mails: bnasri@cds.asal.dz, hbensikadour@cds.asal.dz, abab@cds.asal.dz, sbekkardjelloulsaiah@cds.asal.dz, debabahamed@cds.asal.d, aadnane@cds.asal.dz

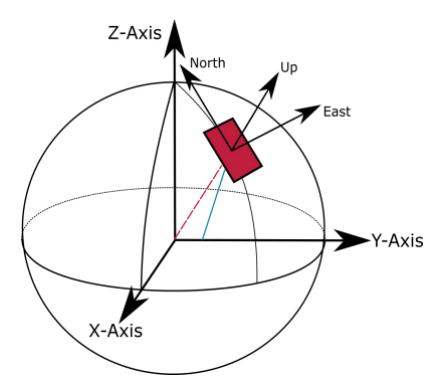


Fig. 1- Relation between ECEF and ENU.

The ECEF coordinate system, also known as the geocentric coordinate system, is a three-dimensional Cartesian coordinate system with its origin at the Earth's center of mass. This system rotates with the Earth, so fixed points on the Earth's surface have constant coordinates.

- X-axis points from the Earth's center towards the intersection of the Equator and the Prime Meridian (0° longitude).
- Y-axis points from the Earth's center towards 90° east longitude.
- Z-axis points from the Earth's center towards the North

The ENU coordinate system is a local tangent plane coordinate system used to describe positions relative to a specific location on the Earth's surface. This system is particularly useful for local observations and operations.

- East (E) axis points towards the east, parallel to the local tangent to the Earth's surface.
- North (N) axis points towards the north, also parallel to the local tangent to the Earth's surface.
- Up (U) axis points away from the Earth's surface, perpendicular to the local tangent plane.

To convert the ECEF coordinates to ENU coordinates, we use the following rotation matrix:

$$\begin{bmatrix} E \\ N \\ U \end{bmatrix} = \begin{bmatrix} -\sin\lambda & \cos\lambda & 0 \\ -\sin\phi\cos\lambda & -\sin\phi\sin\lambda & \cos\phi \\ \cos\phi^*\cos\lambda & \cos\phi\sin\lambda & \sin\phi \end{bmatrix} \begin{bmatrix} x_p - x_r \\ y_p - y_r \\ z_p - z_r \end{bmatrix}$$
(1)

where,  $(x_p, y_p, z_p)$  are the ECEF coordinates of the point,  $(x_r, y_r, z_r)$  are the ECEF coordinates of the reference point (origin of the ENU system) and  $(\varphi)$ ,  $(\lambda)$  represents respectively latitude and longitude for geodetic coordinates of the reference point.

With the ENU coordinates we compute the azimuth (AZ), elevation (EL), and range (R) as follows:

$$AZ = \begin{cases} \operatorname{atan}\left(\frac{y}{x}\right), & \text{if } x > 0, \\ \operatorname{atan}\left(\frac{y}{x}\right) + \pi, & \text{if } x < 0, \\ \frac{\pi}{2} & \text{else.} \end{cases}$$

$$EL = \arccos\left(\frac{z}{R}\right), \tag{3}$$

$$EL = \arccos\left(\frac{z}{R}\right),$$
 (3)

$$R = \sqrt{x^2 + y^2 + z^2}. (4)$$

# 2.2 DOPPLER SHIFT

As a satellite moves relative to the ground station, the frequency of the signal it transmits appears to change. When the satellite is approaching the GS, the frequency increases (blue shift), and when it is moving away, the frequency decreases (red shift) [23]. This effect is crucial to account for in satellite communication systems to ensure accurate signal reception and transmission. It is calculated by:

$$\Delta f = \frac{\pm V_r * f}{f},\tag{5}$$

where,  $V_r$  is the relative speed between satellite and GS, C is the velocity of light and f is the frequency of the transmitted signal.

# 3. PROPOSED ARCHITECTURE

We propose an architecture divided into two modules (software/hardware) represented by dotted lines in Fig. 2.

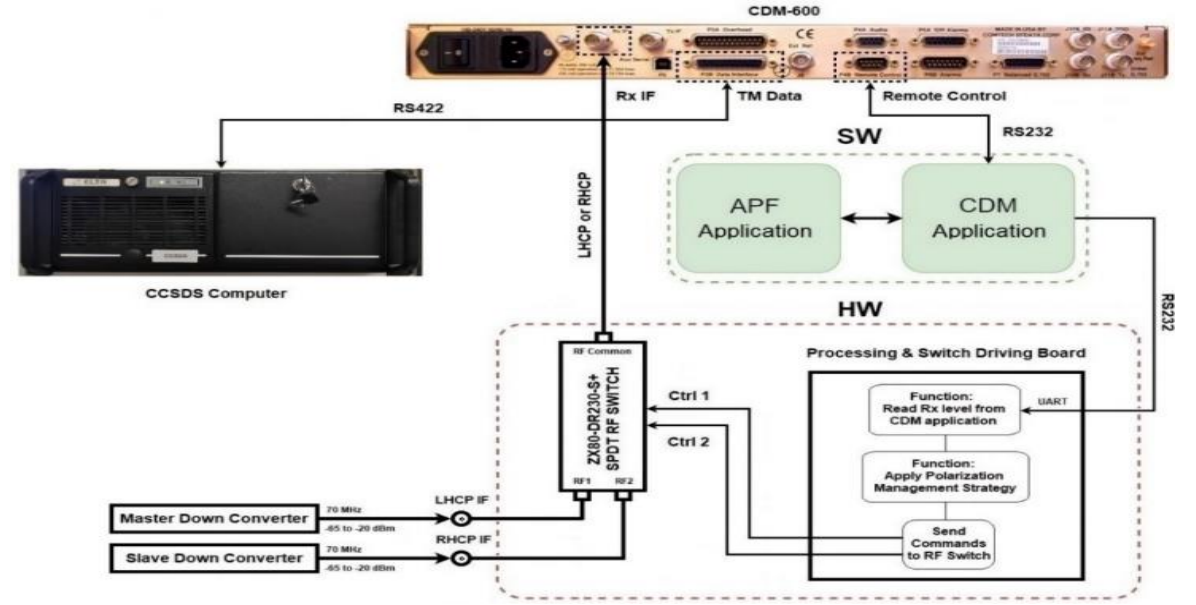


Fig. 2 – Block diagram of the hybrid HW/SW solution.

# 3.1. SOFTWARE COMPONENT

The antenna pointing file (APF) application [17] is based on the simplified general perturbations 4 (SGP4) propagator programmed in Python, its objective is to define and provide to the station the crucial parameters related to the satellite trajectory and the communication frequency. These parameters allow the station to establish a stable connection with the satellite by providing the azimuth and elevation angles necessary to point the antenna, as well as transmitting the Doppler Shift value to adjust the receiving frequency and compensate for the shift caused by relative motion between the satellite and the station.

The CDM application (Fig. 3) is responsible for controlling the CDM-600 demodulator via the RS232 port, configuring its parameters according to the specific characteristics of the satellite to be monitored, such as the type of modulation (BPSK, QPSK, etc.), the type of decoding (Turbo Code, Viterbi, etc.), and the transmission rate, among others, as well as reading the level of the reception signal "Rx Level", information which our polarization management solution will use.



Fig. 3 – CDM-600 Application.

On the other hand, during the passes, a calculation is performed to determine the offset based on the Doppler shift estimated from the APF application and the frequency measured by the demodulator. A new reference frequency is transmitted to the demodulator when the measured offset reaches  $\pm 12~\mathrm{kHz}$ .

# 3.2 HARDWARE COMPONENT

The hardware component includes an RF switch model ZX80-DR230-S+ from Mini-Circuits [24], as well as a control board equipped with an ATMega328P

microcontroller as its core. This board facilitates communication with the CDM application via the RS232 port, implements the functions of reading and applying the polarization management strategy, and provides control of the RF switch.

Fig. 4 represents the flowchart of the proposed solution within the existing architecture of the ALSAT-2 station.

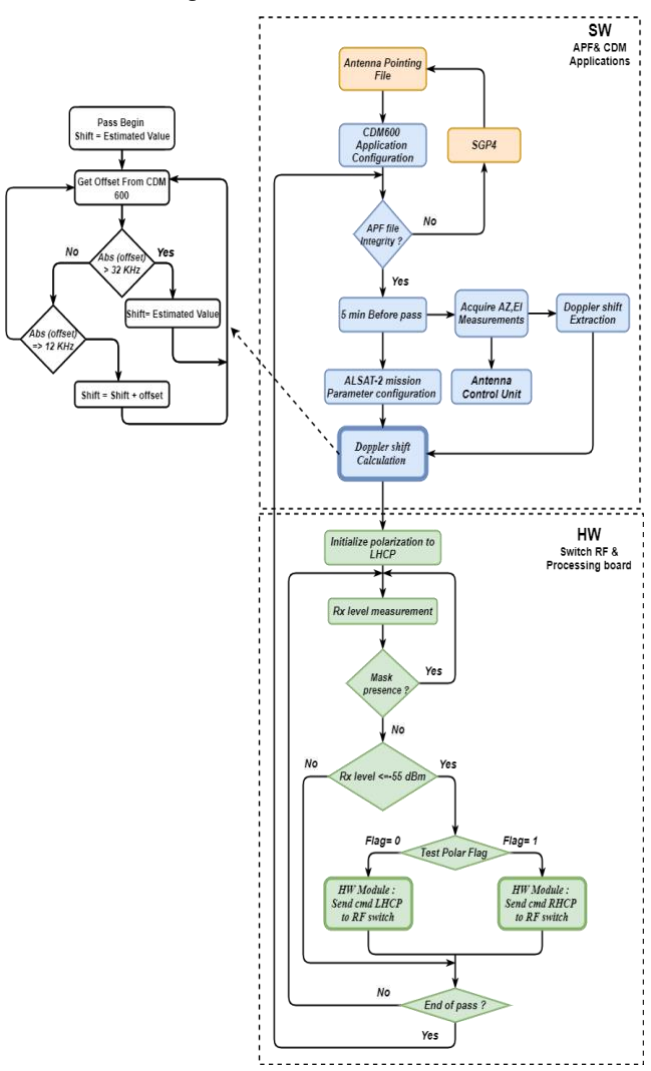
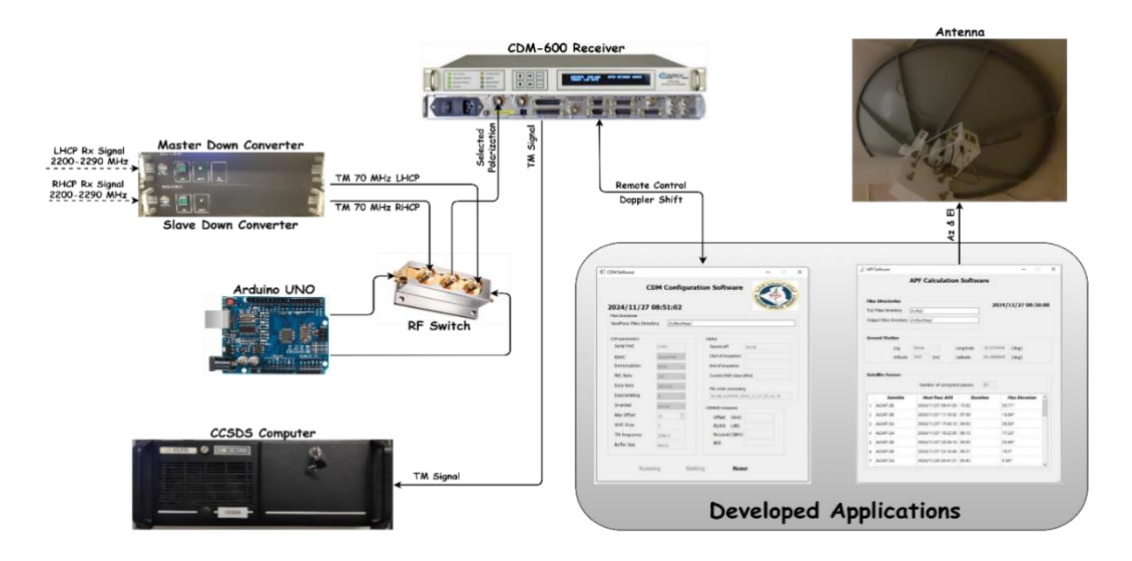


Fig. 4 - Flowchart of the mixed polarization management solution.

# 4. IMPLEMENTATION AND RESULTS

To verify the effectiveness of our method in adjusting the Doppler shift between the ALSAT-2 satellites and the earth station, we have fully implemented the recommended solution on the Oran site for the S band, according to the test configuration presented in Fig. 5. Both satellites evolve in a sun-synchronous circular quasi-polar orbit, with inclinations of 98.7 degrees and 98.9 degrees, altitudes of 645 km and 745 km, respectively for ALSAT-2A and ALSAT-2B. They are 180 degrees apart in orbital phase. Station configuration parameters include a TM frequency of 2266.5 MHz, a TC frequency of 2087.1 MHz, and an intermediate demodulator frequency of 70 MHz. The bit rate is set at 384.615 kb/s.



 $Fig.\ 5-Hardware/Software\ implementation.$ 

# 4.1 TEST WITH AN ALSAT-2A SATELLITE PASS

The azimuth and elevation profiles of the ALSAT-2A pass, followed for this test are illustrated in Fig. 6 and Fig. 7. The characteristics of this pass are as follows:

AOS: 2023/11/08 08:20:48
LOS: 2023/11/08 08:31:05
Maximum elevation: 36.1°

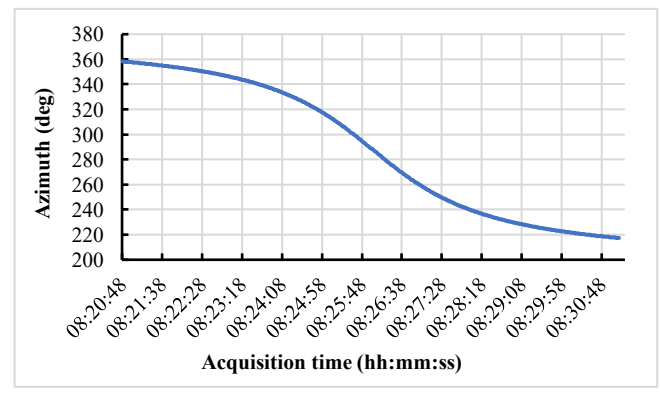


Fig. 6 – ALSAT-2A Pass Azimuth Profile.

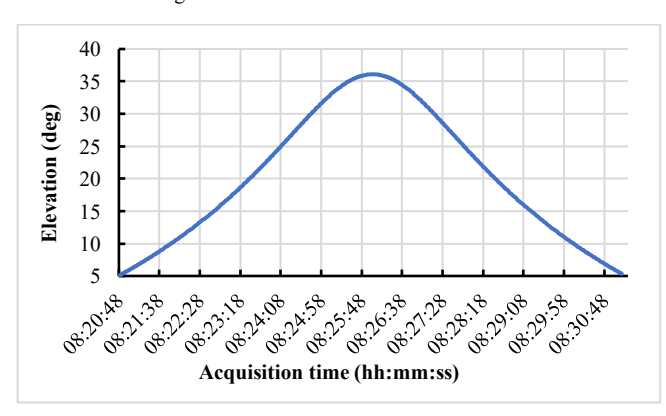


Fig. 7 – ALSAT-2A Pass Elevation Profile.

The Doppler shift values measured by the demodulator during the ALSAT-2A pass match the estimated (Fig. 8), with a difference of 2.2-3.4 kHz (Fig. 9), which is negligible compared to the operating frequency.

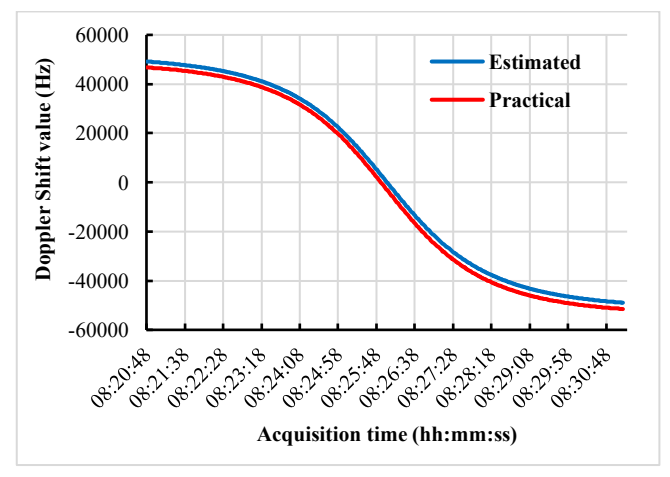


Fig. 8 – Estimated and practical Doppler shift – ALSAT-2A pass.

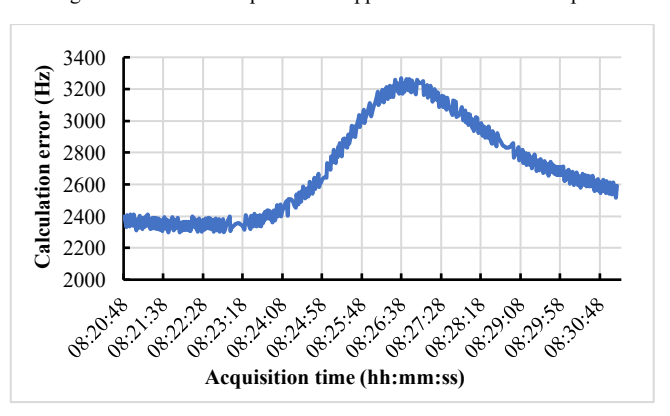


Fig. 9 – Calculation error of Doppler shift – AlSAT-2A pass.

The curve in Fig. 10, relating to the signal level at the "Rx IF" input of the CDM-600, shows the beneficial effect of implementing our solution for managing the two polarizations. In fact, the signal at the equipment's input has a more uniform level for most of the satellite pass. The first encountered signal drop (level at -60 dBm) is caused by the low elevations occurring at the beginning of the pass, the last one is due to the presence of a mask (building obstructing the signal). The Eb/N0 parameter (Fig. 11), which measures signal quality, follows a trend practically identical to that of the "Rx Level".



Fig. 10 - Rx level - AlSAT-2A pass.



Fig. 11 – Eb/N0 – ALSAT-2A pass.

# 4.2 TEST WITH AN ALSAT-2B SATELLITE PASS

The azimuth and elevation profiles of the ALSAT-2B pass, followed for this test, are illustrated in Fig. 12 and Fig. 13. The characteristics of this pass are as follows:

AOS: 2023/11/08 09:02:23
LOS: 2023/11/08 09:12:02
Maximum elevation: 21.51°



 $Fig.\ 12-ALSAT\text{-}2B\ Pass\ Azimuth\ Profile.$ 

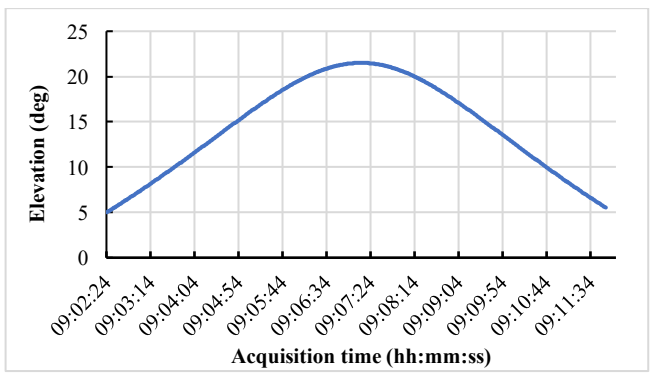


Fig. 13 – ALSAT-2B pass elevation profile.

As with the ALSAT-2A passes, the Doppler shift compensation algorithm allows for a good match between the Doppler shift values measured during the ALSAT-2B passes and those estimated (Fig. 14), with a difference ranging from 2.9 kHz to 4.5 kHz (Fig. 15).

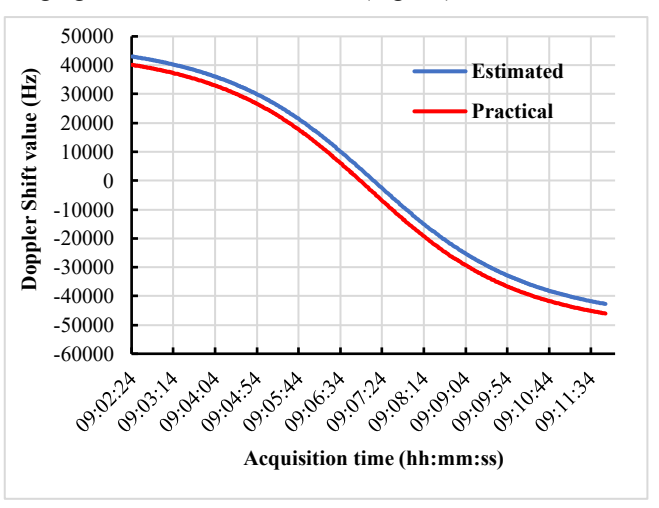


Fig. 14 - Estimated and practical Doppler shift - ALSAT-2B pass.

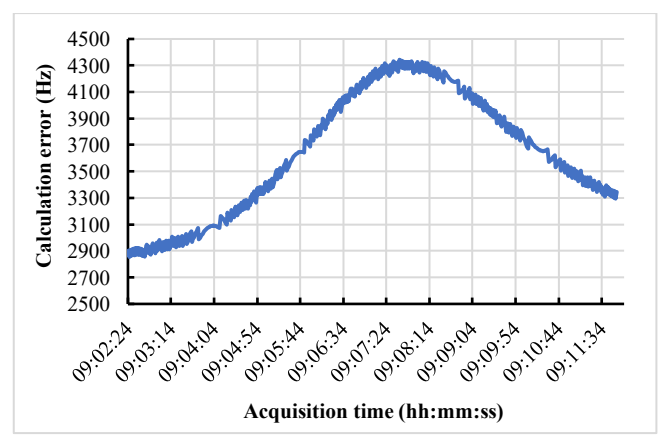


Fig. 15 – Calculation error of Doppler shift – AlSAT-2B pass.

As for the test with the ALSAT-2A satellite, the one carried out with a pass of the ALSAT-2B satellite confirms the advantage provided by our polarization management solution, with a fairly stable signal level (Fig. 16) and quality (Fig. 17), if we except the beginnings and ends of passes as well as the effect of the presence of a mask, if applicable.

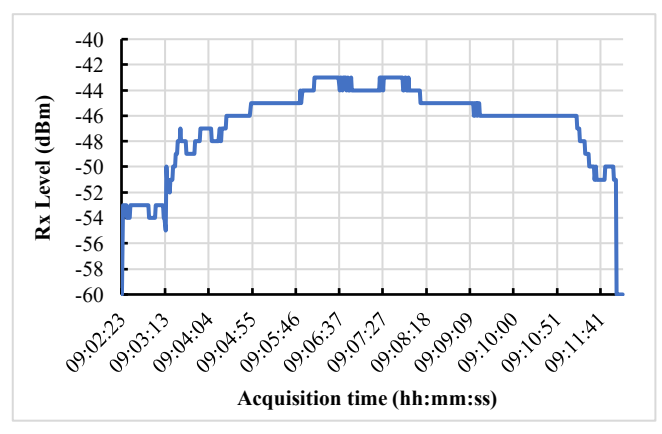


Fig. 16 - Rx Level - AlSAT-2B pass.

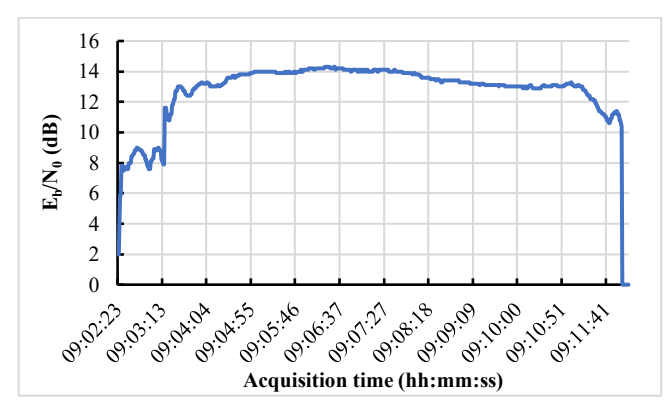


Fig. 17 - Eb/N0 - ALSAT-2B Pass.

The average Eb/N0 values and Rx levels for the ALSAT-2A and ALSAT-2B passes are reported in the table below.

Table 1  $E_b/N_0$  and Rx average

20110 and 121 a votago			
ALSAT-2A	$E_b/N_0$ , dB	10,83	
	Rx level, dBm	-49,96	
ALSAT-2B	$E_b/N_0$ , dB	12,82	
	Rx level, dBm	-46.43	

# 5. CONCLUSION

The results of our experiments confirm that the solution implemented in the Oran S-band station can be practically operated with the communication systems of the ALSAT-2A and ALSAT-2B satellites in low Earth orbit. As part of this work, we first identified potential limitations in the station's architecture, then carried out the necessary hardware and software development to communicate stably with these two satellites, with efficient Doppler shift management and without telemetry loss at the ground segment.

For future work, it would be relevant to extend this approach to other missions, such as ALSAT-1B, to evaluate the adaptability and robustness of the proposed solution across different orbital configurations and communication scenarios.

# CREDIT AUTHORSHIP CONTRIBUTION STATEMENT

Boualem Nasri: Propose the solution and system design, results analysis, and writing.

El Habib Bensikaddour: Development of APF and CDM-600 applications, review writing.

Amine Bab: Development of Hardware implementation, Testing.
Saiah Bekkar Djelloul Saiah: Contribution to experimental setup.
Djamel Eddine Baba Hamed: Experimental setup, review writing, Testing.
Akram Adnane: Contribution to experimental setup

Received on 8 August 2024.

# REFERENCES

- L. Antiufrieva et al., Features of frequency synchronization algorithms DVB-S2 (X) for LEO satellites, In 2021 23rd International Conference on Digital Signal Processing and its Applications (DSPA), IEEE (2021).
- J.E. Benmansour and B. Khouane, Feed-forward control design for roll/yaw attitude flexible spacecraft based on the disturbance observer, Rev. Roum. Sci. Techn. – Électrotechn. et Énerg., 67, 2, pp. 187–191 (2022).

- J.E. Benmansour, R. Roubache, B. Khouane, and N. Bekhadda, Robust attitude controller and fault detection of flexible satellite, Rev. Roum. Sci. Techn. – Électrotechn. et Énerg., 70, 1, pp. 121–126 (2025).
- O. Nia and B.L. Mark, Models for frequency doppler shift prediction for LEO satellites at L-band, Military Communications Conference (MILCOM), IEEE (2022).
- E.G. Peters, K. Day, and C.R. Benson, A real-time Doppler compensating physical/data link layer protocol for satellite communications, In 2020 IEEE Aerospace Conference, IEEE (2020).
- E.G. Peters and C.R. Benson, A Doppler correcting software defined radio receiver design for satellite communications, IEEE Aerospace and Electronic Systems Magazine, 35, 2, pp. 38–48 (2020).
- M.Z. Baba-Ahmed, R.D. Taleb, M.A. Rabah, S. Benabbou, and M.I. Soufi, *Hybrid design patch antenna for X-band satellite communication*, Rev. Roum. Sci. Techn. Electrotechn. et Énerg., 70, 3, pp. 379–384 (2025).
- 8. A. Aloman, M.P. Garcia, I. Nicolaescu, F. Popescu, and L. Buzincu, Circularly polarized periodic leaky-wave antenna based on a coaxial line with helical slot, Rev. Roum. Sci. Techn. Électrotechn. et Énerg., 70, 1, pp. 87–90 (2025).
- M. Katayama, A. Ogawa, and N. Morinaga, Carrier synchronization under Doppler shift of the nongeostationary satellite communication systems, Proceedings Singapore ICCS/ISITA92, IEEE (1992).
- J.-J. Van de Beek, M. Sandell, and P.O. Borjesson, ML estimation of time and frequency offset in OFDM systems, IEEE Transactions on Signal Processing, 45, 7, pp. 1800–1805 (1997).
- I. Ali, N. Al-Dhahir, and J.E. Hershey, *Doppler characterization for LEO satellites*, IEEE Transactions on Communications, 46, 3, pp. 309–313 (1998).
- 12. I. Ali et al., Doppler applications in LEO satellite communication systems, Vol. 656, Springer Science & Business Media (2005).
- S. Bekkar Djelloul Saiah et al., Analysis of the communication links between the AlSat-1b satellite and the ground station: The impact of the Auto Tracking system on antenna pointing accuracy, International Journal of Satellite Communications and Networking, 39, 5, pp. 486–499 (2021).
- C.H. Cho et al., Antenna control system using step tracking algorithm with H∞ controller, International Journal of Control, Automation, and Systems, 1, 1, pp. 83–92 (2003).
- D. Nieto YII, Doppler shift compensation strategies for LEO satellite communication systems, Universitat Politècnica de Catalunya (2018).
- H. Rouzegar, M. Nasirian, and M. Ghanbarisabagh, Novel algorithm for tracking LEO satellites using Doppler frequency shift technique, Wireless Personal Communications, 96, pp. 2161–2178 (2017).
- E. Bensikaddour et al., Azimuth, elevation, and Doppler shift estimation for LEO satellites based on an open source Python package, Automatic Control and Computer Sciences, 57, 2, pp. 203–212 (2023).
- C. Cao and S. Zhai, The influence of LEO satellite Doppler effect on LoRa modulation and its solution, In Journal of Physics: Conference Series, IOP Publishing (2021).
- 19. A. Al-Hourani and B. Al Homssi, *Doppler shift distribution in satellite constellations*, IEEE Communications Letters (2024).
- A. Bab et al., hybrid implementation of a Doppler shift compensation solution for LEO satellite communication systems, International Symposium on Electronics and Telecommunications (ISETC), Timisoara, Romania, pp. 1–5 (2024).
- 21. \*\*\*Comtech EF Data, CDM-600 Satellite Modem (2024).
- J.M. Gongora-Torres et al., Elevation angle characterization for LEO satellites: First and second order statistics, Applied Sciences, 13, 7, 4405 (2023).
- J. Mass and E. Vassy, Doppler effect of artificial satellites, In Advances in Space Science and Technology, Elsevier, pp. 1–38 (1962).
- in Space Science and Technology, Elsevier, pp. 1–38 (1962).

  24. Mini-Circuits, ZX80-DR230-S+ RF amplifier (2024). Available: https://www.minicircuits.com/pdfs/ZX80-DR230+.pdf?srsltid=AfmBOoqP2RYWioZNBWZihsQH4gSQPQuA4iFcqcaHxMDqTLzh4sMM-TUk.